Journal of
Mechanics of
Materials and Structures

AN ANISOTROPIC PIEZOELECTRIC HALF-PLANE CONTAINING AN ELLIPTICAL HOLE OR CRACK SUBJECTED TO UNIFORM IN-PLANE ELECTROMECHANICAL LOADING

Ming Dai, Peter Schiavone and Cun-Fa Gao

Volume 11, No. 4 July 2016

msp

JOURNAL OF MECHANICS OF MATERIALS AND STRUCTURES
Vol. 11, No. 4, 2016
dx.doi.org/10.2140/jomms.2016.11.433

AN ANISOTROPIC PIEZOELECTRIC HALF-PLANE CONTAINING AN ELLIPTICAL HOLE OR CRACK SUBJECTED TO UNIFORM IN-PLANE ELECTROMECHANICAL LOADING

MING DAI, PETER SCHIAVONE AND CUN-FA GAO

We derive a series solution for the electro-elastic field inside an anisotropic piezoelectric half-plane containing an elliptical hole or a crack when the half-plane is subjected to in-plane mechanical and electric loadings. Our solution is based on a specific type of conformal map which allows for the mapping of a complete half-plane (without a hole) onto the interior of the unit circle in the imaginary plane. We illustrate our solution with several examples. We show that with decreasing distance between the hole and the edge of the half-plane, the maximum hoop stress around the hole increases rapidly under mechanical loading but slowly in the presence of electric loading. In particular, for a crack with particular orientation in a piezoelectric half-plane subjected to pure shear, we find that the mode-II stress intensity factor at the crack tip farthest from the edge of the half-plane may decrease as the crack approaches the edge. Moreover, if the distance between the crack or the elliptical hole and the edge of the half-plane exceeds four times the size of the hole or semi-length of the crack, the half-plane can be treated essentially as a whole plane without inducing significant errors in the stress concentration around the hole or in the stress and electric displacement intensity factors at the crack tips.

1. Introduction

Piezoelectric materials have been used widely in electronic and mechatronic devices due to their pronounced electromechanical coupling properties. However, since various defects (e.g. pores, micro-cracks or inclusions) often arise in the manufacture of piezoelectric materials, high stress and/or electric field concentrations may be induced near defects when the material is subjected to mechanical and/or electric loading. This, in turn, may cause crack initialization/growth, dielectric breakdown, fracture and ultimately failure [Zhang and Gao 2004]. In an effort to predict the reliability of piezoelectric devices, problems involving the prediction of electro-elastic fields (including stress and electric field concentrations) in piezoelectric materials containing holes or inclusions have attracted tremendous attention in the literature. In the context of two-dimensional deformations, researchers have examined problems involving the anti-plane shear of an isotropic plane of the piezoelectric material subjected to out-of-plane shear loading and in-plane electric loading as well as plane strain or plane stress problems corresponding to an anisotropic plane of the piezoelectric material subjected to both in-plane mechanical and electric loading. In the case of anti-plane shear, analytical results have been obtained not only for the case of an elliptical hole/inclusion [Pak 2010; Guo et al. 2010] but also for an arbitrarily-shaped hole/inclusion [Shen et al. 2010; Wang and Zhou 2013; Wang et al. 2015]. Problems involving plane strain or plane stress are rather more challenging with analytical methods available only when the hole/inclusion is

Keywords: elliptical hole, crack, piezoelectric material, half-plane.

elliptical [Sosa 1991; Sosa and Khutoryansky 1996; Chung and Ting 1996; Qin 1998; Gao and Fan 1999; Wang and Gao 2012] (see, in particular, the explanation in [Ting 2000]) with most studies resorting to approximate methods to deal with cases of non-elliptical holes/inclusions [Dai and Gao 2014].

In many piezoelectric systems (structures or composites), it is common for holes or inclusions to appear near an edge. This suggests that the system could be adequately modelled as a half-plane (rather than a whole plane) containing holes or inclusions. In this context, Ru [2000] and Pan [2004] have obtained exact solutions for a piezoelectric half-plane containing an arbitrarily-shaped inclusion and a polygonal inclusion with uniform eigenstrains, respectively. However, in both of [Ru 2000; Pan 2004], the solutions require that the inclusion has the same material constants as those of its surrounding piezoelectric matrix (this essentially prevents the inclusion from degenerating into a hole). Kaloerov and Glushchenko [2001] derived an approximate solution for a piezoelectric half-plane with holes or cracks using a collocation method to deal with the boundary conditions on the holes/cracks. It is well-known, however, that collocation methods often produce unsatisfactory and imprecise results with convergence often becoming unstable with an increasing number of collocation points resulting in the possibility that the corresponding boundary conditions are not well-satisfied. Based on the fundamental solution for a dislocation in a piezoelectric half-plane, Yang et al. [2007] obtained a general solution for a crack in a piezoelectric half-plane with a traction-induction free surface by modeling the crack using continuously distributed dislocations. However, it is extremely difficult to extend the method in [Yang et al. 2007] to deal with the equally significant case of a hole in a half-plane. In particular, we mention that, despite the fact that an internal electric field inside the hole or crack may induce a significant impact on the surrounding electro-elastic field and subsequently on the fracture behavior of the corresponding materials (see [Sosa and Khutoryansky 1996; Gao and Fan 1999]), the contribution of any internal electric field remains absent from both aforementioned papers [Kaloerov and Glushchenko 2001; Yang et al. 2007]. In this paper, recognizing the above-mentioned deficiencies in the methods used previously, we develop a new efficient method, completely distinct from those used in [Kaloerov and Glushchenko 2001; Yang et al. 2007] to address the problem of plane strain deformations of a piezoelectric half-plane containing an elliptical hole or crack. In particular, we incorporate the contribution of electromechanical loadings applied on surface of the half-plane and assume that the elliptical hole is permeable to an electric field. This further requires that we take into consideration the electric field inside the hole: an issue hitherto absent in the problem of a general anisotropic half-plane containing an elliptical hole.

The paper is organized as follows. Basic formula and boundary conditions of the problem are presented in Section 2. The details of a novel solution procedure are given in Section 3. In Section 4, we calculate the stress concentration around the elliptical hole and the electro-elastic intensity factors at the crack tips. Finally, the main results are summarized in Section 5.

2. Basic formula and boundary conditions

We refer to the standard Cartesian xy-coordinate system and consider the plane strain deformation of a piezoelectric lower half-plane containing an elliptical hole (see Figure 1 which includes the geometrical parameters of the hole) whose poling direction is along the positive y-axis. The elliptical hole degenerates into a crack when the minor axis of the elliptical hole tends towards zero. It is assumed that uniform mechanical loadings $(\sigma_{xx}^{\infty}, \sigma_{yy}^{\infty}, \sigma_{xy}^{\infty})$ and uniform electric displacement loadings $(D_x^{\infty}, D_y^{\infty})$ are applied

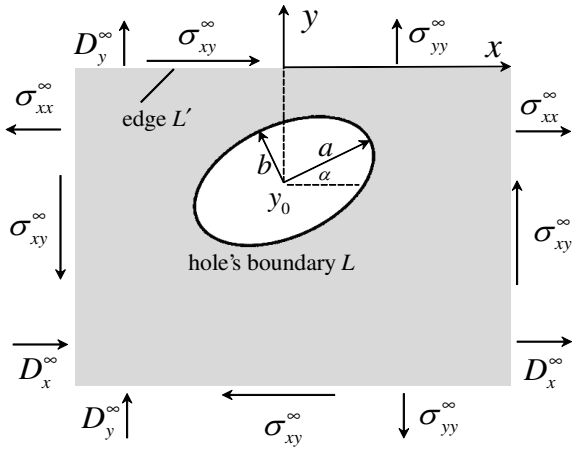

Figure 1. A piezoelectric half-plane with an elliptical hole.

both at infinity and on the edge L' of the half-plane and that the elliptical hole has a traction-free boundary and is filled with a homogeneous gas or liquid with dielectric constant ϵ_0. The stress components $(\sigma_{xx}, \sigma_{yy}, \sigma_{xy})$, the electric displacement components (D_x, D_y) and the electric potential ϕ of the piezoelectric half-plane can be described in terms of three complex functions $\varphi_i(z_i)$ $(z_i = x + \mu_i y, i = 1, 2, 3)$ as [Sosa 1991]

$$\langle \sigma_{xx}, \sigma_{yy}, \sigma_{xy} \rangle = \quad 2\mathrm{Re}\left\{ \sum_{i=1}^{3} \langle \mu_i^2, 1, -\mu_i \rangle \varphi_i'(z_i) \right\}, \tag{1}$$

$$\langle D_x, D_y \rangle = \quad 2\mathrm{Re}\left\{ \sum_{i=1}^{3} \lambda_i \langle \mu_i, -1 \rangle \varphi_i'(z_i) \right\}, \tag{2}$$

$$\phi = -2\mathrm{Re}\left\{ \sum_{i=1}^{3} \kappa_i \varphi_i'(z_i) \right\} \tag{3}$$

where the angled brackets represent vectors and the related constants $(\mu_i, \lambda_i, \kappa_i)$ are determined by the elastic constants a_{ij}, piezoelectric constants b_{ij} and dielectric constants c_{ij} of the piezoelectric material occupying the half-plane, as [Sosa 1991]

$$\begin{aligned} &a_{11}c_{11}\mu_i^6 + (a_{11}c_{22} + 2a_{12}c_{11} + a_{33}c_{11} + b_{21}^2 + b_{13}^2 + 2b_{21}b_{13})\mu_i^4 + \\ &(a_{22}c_{11} + 2a_{12}c_{22} + a_{33}c_{22} + 2b_{21}b_{22} + 2b_{13}b_{22})\mu_i^2 + a_{22}c_{22} + b_{22}^2 = 0, \end{aligned} \tag{4}$$

$$\lambda_i = -\frac{(b_{21} + b_{13})\mu_i^2 + b_{22}}{c_{11}\mu_i^2 + c_{22}}, \quad \kappa_i = (b_{13} + c_{11}\lambda_i)\mu_i. \tag{5}$$

Here, μ_i $(i = 1, 2, 3)$ are three distinct complex roots with positive imaginary parts each determined from Equation (4). Figure 2 shows the domains of definition of the functions $\varphi_i(z_i)$ $(i = 1, 2, 3)$, respectively, in which the curves L_i in the z_i-planes $(i = 1, 2, 3)$ correspond to the hole's boundary L in the xy-plane while the edges L_i' in the z_i-planes $(i = 1, 2, 3)$ correspond to the edge L' in the xy-plane.

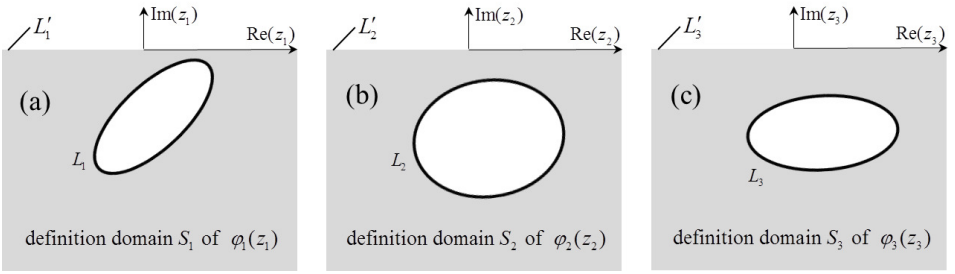

Figure 2. Domain of definition of the complex functions $\varphi_i(z_i)$ $(i = 1, 2, 3)$.

The electric displacement components $(D_x^{(0)}, D_y^{(0)})$ and electric potential $\phi^{(0)}$ of the medium inside the elliptical hole can be expressed in terms of a holomorphic function $f(z)$ ($z = x + Iy$ with I denoting the imaginary unit) by

$$\phi^{(0)} = \mathrm{Re}[f(z)], \tag{6}$$

$$D_x^{(0)} - I D_y^{(0)} = -\epsilon_0 f'(z). \tag{7}$$

Using the functions $\varphi_i(z_i)$ $(i = 1, 2, 3)$ and $f(z)$, the electro-elastic conditions on the hole's boundary L and on the edge L' of the half-plane are then described as [Sosa 1991; Sosa and Khutoryansky 1996]

$$\left.\begin{aligned} 2\mathrm{Re}\left\{\sum_{i=1}^{3}\varphi_i(z_i)\right\} &= B \\ 2\mathrm{Re}\left\{\sum_{i=1}^{3}\mu_i\varphi_i(z_i)\right\} &= C \\ 2\mathrm{Re}\left\{\sum_{i=1}^{3}\lambda_i\varphi_i(z_i)\right\} &= D - \epsilon_0\mathrm{Im}[f(z)] \\ -2\mathrm{Re}\left\{\sum_{i=1}^{3}\kappa_i\varphi_i(z_i)\right\} &= E + \mathrm{Re}[f(z)] \end{aligned}\right\} (z_i \in L_i, z \in L), \tag{8}$$

$$\left.\begin{aligned} 2\mathrm{Re}\left\{\sum_{i=1}^{3}\varphi_i(z_i)\right\} &= B' + \sigma_{yy}^{\infty}x \\ 2\mathrm{Re}\left\{\sum_{i=1}^{3}\mu_i\varphi_i(z_i)\right\} &= C' - \sigma_{xy}^{\infty}x \\ 2\mathrm{Re}\left\{\sum_{i=1}^{3}\lambda_i\varphi_i(z_i)\right\} &= D' - D_y^{\infty}x \end{aligned}\right\} (z_i \in L_i', x \in L') \tag{9}$$

where B, C, D, E, B', C' and D' are real constants to be determined (although they do not influence the final electro-elastic field of the half-plane). In what follows, we determine the four complex functions

$\varphi_i(z_i)$ $(i = 1, 2, 3)$ and $f(z)$ in their respective domains of definition from the boundary conditions (8) and (9).

3. Solution process

3.1. ***Series representations of the complex functions.*** Noting that uniform electro-elastic loadings are imposed at infinity and on the edge of the half-plane, the complex functions $\varphi_i(z_i)$ $(i = 1, 2, 3)$ can take the form

$$\varphi_i(z_i) = A_i z_i + \varphi_{i0}(z_i), \quad i = 1, 2, 3; \tag{10}$$

where $\varphi_{i0}(z_i)$ $(i = 1, 2, 3)$ are holomorphic in the regions S_i $(i = 1, 2, 3$; see Figure 2), respectively, while the complex constants A_i $(i = 1, 2, 3)$ are specified by the imposed electro-elastic loadings (according to Equations (1) and (2)) as

$$\begin{aligned} \langle \sigma_{xx}^{\infty}, \sigma_{yy}^{\infty}, \sigma_{xy}^{\infty} \rangle &= 2\mathrm{Re}\left\{ \sum_{i=1}^{3} \langle \mu_i^2, 1, -\mu_i \rangle A_i \right\}, \\ \langle D_x^{\infty}, D_y^{\infty} \rangle &= 2\mathrm{Re}\left\{ \sum_{i=1}^{3} \lambda_i \langle \mu_i, -1 \rangle A_i \right\}. \end{aligned} \tag{11}$$

Here, since Equation (11) is insufficient to determine all three complex constants A_i $(i = 1, 2, 3)$, we can prescribe, for example, $\mathrm{Im}(A_1) = 0$. Note that the domain of definition S_i $(i = 1, 2, 3)$ of each complex function $\varphi_{i0}(z_i)$ $(i = 1, 2, 3)$ can be interpreted as the intersection of an infinite region outside the hole bounded by L_i $(i = 1, 2, 3)$ in the entire z_i-plane $(i = 1, 2, 3)$ and a complete lower z_i-half-plane $(i = 1, 2, 3)$ (without a hole), so that based on the principle of superposition [Dai and Gao 2014; Dai and Sun 2013], $\varphi_{i0}(z_i)$ $(i = 1, 2, 3)$ can be expressed as

$$\varphi_{i0}(z_i) = \sum_{j=1}^{+\infty} a_{i,j} \xi_i^{-j} + \sum_{j=1}^{+\infty} b_{i,j} \eta_i^{j}, \quad i = 1, 2, 3; \tag{12}$$

where $a_{i,j}$ and $b_{i,j}$ are some constant coefficients to be determined. We note that the ξ_i-plane and η_i-plane $(i = 1, 2, 3)$ are associated with the z_i-plane $(i = 1, 2, 3)$ by the following conformal mappings [Lekhnitskii 1950; Copson 1935],

$$\begin{aligned} z_i = \omega_i(\xi_i) &= \mu_i y_0 + \frac{a_0 - I\mu_i b_0}{2}\xi_i + \frac{\bar{a}_0 + I\mu_i \bar{b}_0}{2}\xi_i^{-1}, \quad |\xi_i| \geq 1, \\ a_0 &= a\cos\alpha + Ib\sin\alpha, \quad b_0 = b\cos\alpha + Ia\sin\alpha, \quad i = 1, 2, 3; \end{aligned} \tag{13}$$

$$z_i = \rho(\eta_i) = -Iy_0 \frac{\eta_i + 1}{\eta_i - 1}, \quad |\eta_i| \leq 1, \quad i = 1, 2, 3. \tag{14}$$

Note that (13) maps the infinite region outside the curve L_i $(i = 1, 2, 3)$ in the entire z_i-plane $(i = 1, 2, 3)$

onto the exterior of the unit circle in the ξ_i-plane ($i = 1, 2, 3$), respectively, while (14) maps the complete lower z_i-half-plane ($i = 1, 2, 3$) onto the interior of the unit circle in the η_i-plane ($i = 1, 2, 3$), respectively. In particular, when point (x, y) is located on the hole's boundary L or on the edge L' in the physical xy-plane, the arguments z_i, ξ_i and η_i ($i = 1, 2, 3$) in their respective planes take the values

$$z_i = \begin{cases} \omega_i(\sigma), (z_i \in L_i) \\ \rho(\sigma') = x, (x \in L, z_i \in L_i') \end{cases}, i = 1, 2, 3; \tag{15}$$

$$\xi_i = \begin{cases} \sigma, (z_i \in L_i) \\ \omega_i^{-1}(\rho(\sigma')), (|\omega_i^{-1}(\rho(\sigma'))| > 1, z_i \in L_i') \end{cases}, i = 1, 2, 3; \tag{16}$$

$$\eta_i = \begin{cases} \rho^{-1}(\omega_i(\sigma)), (z_i \in L_i) \\ \sigma', (z_i \in L_i') \end{cases}, i = 1, 2, 3; \tag{17}$$

with

$$\begin{aligned} \sigma &= e^{I\theta}, \quad 0 \le \theta \le 2\pi, \\ \sigma' &= e^{I\theta'}, \quad 0 \le \theta' \le 2\pi. \end{aligned} \tag{18}$$

Consequently on the curves L_i ($i = 1, 2, 3$) and L_i' ($i = 1, 2, 3$) in the z_i-plane ($i = 1, 2, 3$), the complex functions $\varphi_i(z_i)$ ($i = 1, 2, 3$) can be expressed completely with respect to the arguments σ and σ', respectively, as

$$\varphi_i(z_i) = A_i\omega_i(\sigma) + \sum_{j=1}^{+\infty} a_{i,j}\sigma^{-j} + \sum_{j=1}^{+\infty} b_{i,j}[\rho^{-1}(\omega_i(\sigma))]^j, \quad z_i \in L_i, \quad i = 1, 2, 3; \tag{19}$$

$$\varphi_i(z_i) = A_i\rho(\sigma') + \sum_{j=1}^{+\infty} a_{i,j}[\omega_i^{-1}(\rho(\sigma'))]^{-j} + \sum_{j=1}^{+\infty} b_{i,j}(\sigma')^j, \quad z_i \in L_i', \quad i = 1, 2, 3. \tag{20}$$

On the other hand, since the function $f(z)$ is defined in the region occupied by the elliptical hole in the physical xy-plane, it can be expanded into a Faber series such as [Dai and Sun 2013]

$$\begin{gathered} f(z) = \sum_{j=1}^{+\infty} c_j(a+b)^{-j}\left[\left(P + \sqrt{P^2 - a^2 + b^2}\right)^j + \left(P - \sqrt{P^2 - a^2 + b^2}\right)^j\right], \\ P = (z - Iy_0)e^{-I\alpha}, \end{gathered} \tag{21}$$

where the c_j are constant coefficients to be determined. Specifically, the boundary value of $f(z)$ on the curve L in the xy-plane turns out to be

$$f(z) = \sum_{j=1}^{+\infty} c_j\left[\sigma^j + \left(\frac{a-b}{a+b}\right)^j \sigma^{-j}\right], \quad \sigma = e^{I\theta}, \quad z \in L \tag{22}$$

where σ is given in Equation (18).

3.2. ***Fourier expansion method.*** Substituting (19), (20) and (22) into the boundary conditions (8) and (9) we obtain

$$
\begin{aligned}
&2\mathrm{Re}\left\{\sum_{i=1}^{3}\left[A_i\omega_i(\sigma)+\sum_{j=1}^{+\infty}a_{i,j}\sigma^{-j}+\sum_{j=1}^{+\infty}b_{i,j}[\rho^{-1}(\omega_i(\sigma))]^j\right]\right\}=B,\\
&2\mathrm{Re}\left\{\sum_{i=1}^{3}\mu_i\left[A_i\omega_i(\sigma)+\sum_{j=1}^{+\infty}a_{i,j}\sigma^{-j}+\sum_{j=1}^{+\infty}b_{i,j}[\rho^{-1}(\omega_i(\sigma))]^j\right]\right\}=C,\\
&2\mathrm{Re}\left\{\sum_{i=1}^{3}\lambda_i\left[A_i\omega_i(\sigma)+\sum_{j=1}^{+\infty}a_{i,j}\sigma^{-j}+\sum_{j=1}^{+\infty}b_{i,j}[\rho^{-1}(\omega_i(\sigma))]^j\right]\right\}\\
&\qquad=D-\epsilon_0\mathrm{Im}\left\{\sum_{j=1}^{+\infty}c_j\left[\sigma^j+\left(\frac{a-b}{a+b}\right)^j\sigma^{-j}\right]\right\},\\
&-2\mathrm{Re}\left\{\sum_{i=1}^{3}\kappa_i\left[A_i\omega_i(\sigma)+\sum_{j=1}^{+\infty}a_{i,j}\sigma^{-j}+\sum_{j=1}^{+\infty}b_{i,j}[\rho^{-1}(\omega_i(\sigma))]^j\right]\right\}\\
&\qquad=E+\mathrm{Re}\left\{\sum_{j=1}^{+\infty}c_j\left[\sigma^j+\left(\frac{a-b}{a+b}\right)^j\sigma^{-j}\right]\right\},
\end{aligned}
\tag{23}
$$

and

$$
\begin{aligned}
&2\mathrm{Re}\left\{\sum_{i=1}^{3}\left[\sum_{j=1}^{+\infty}a_{i,j}[\omega_i^{-1}(\rho(\sigma'))]^{-j}+\sum_{j=1}^{+\infty}b_{i,j}(\sigma')^j\right]\right\}=B',\\
&2\mathrm{Re}\left\{\sum_{i=1}^{3}\mu_i\left[\sum_{j=1}^{+\infty}a_{i,j}[\omega_i^{-1}(\rho(\sigma'))]^{-j}+\sum_{j=1}^{+\infty}b_{i,j}(\sigma')^j\right]\right\}=C',\\
&2\mathrm{Re}\left\{\sum_{i=1}^{3}\lambda_i\left[\sum_{j=1}^{+\infty}a_{i,j}[\omega_i^{-1}(\rho(\sigma'))]^{-j}+\sum_{j=1}^{+\infty}b_{i,j}(\sigma')^j\right]\right\}=D'.
\end{aligned}
\tag{24}
$$

Note that both sides of Equations (23) and (24) can be expanded into Fourier series in σ, and σ', respectively. Consequently, if we truncate the series in Equations (12) and (21) so that we seek only the unknown coefficients $a_{i,j}$ $(i=1,2,3;\ j=1\ldots N)$, $b_{i,j}$ $(i=1,2,3;\ j=1\ldots M)$ and c_j $(j=1\ldots N)$, equating the coefficients of σ^k $(k=1\ldots N)$ and $(\sigma')^k$ $(k=1\ldots M)$ on both sides of Equations (23) and (24), respectively, we obtain a system of linear equations with respect to the unknown coefficients $a_{i,j}$ $(i=1,2,3;\ j=1\ldots N)$, c_j $(j=1\ldots N)$ and $b_{i,j}$ $(i=1,2,3;\ j=1\ldots M)$, namely

$$\left.\begin{aligned}
&\sum_{i=1}^{3}\left[A_i C_{i,k}^{(2)}+\bar{A}_i\bar{C}_{i,-k}^{(2)}+\sum_{j=1}^{M}b_{i,j}C_{i,j,k}^{(1)}+\sum_{j=1}^{M}\bar{b}_{i,j}\bar{C}_{i,j,-k}^{(1)}+\bar{a}_{i,k}\right]=0,\\
&\sum_{i=1}^{3}\mu_i\left[A_i C_{i,k}^{(2)}+\bar{A}_i\bar{C}_{i,-k}^{(2)}+\sum_{j=1}^{M}b_{i,j}C_{i,j,k}^{(1)}+\sum_{j=1}^{M}\bar{b}_{i,j}\bar{C}_{i,j,-k}^{(1)}+\bar{a}_{i,k}\right]=0,\\
&\sum_{i=1}^{3}\lambda_i\left[A_i C_{i,k}^{(2)}+\bar{A}_i\bar{C}_{i,-k}^{(2)}+\sum_{j=1}^{M}b_{i,j}C_{i,j,k}^{(1)}+\sum_{j=1}^{M}\bar{b}_{i,j}\bar{C}_{i,j,-k}^{(1)}+\bar{a}_{i,k}\right]\\
&\qquad=0.5I\epsilon_0\left[c_k-\left(\frac{a-b}{a+b}\right)^k\bar{c}_k\right],\\
&-\sum_{i=1}^{3}\kappa_i\left[A_i C_{i,k}^{(2)}+\bar{A}_i\bar{C}_{i,-k}^{(2)}+\sum_{j=1}^{M}b_{i,j}C_{i,j,k}^{(1)}+\sum_{j=1}^{M}\bar{b}_{i,j}\bar{C}_{i,j,-k}^{(1)}+\bar{a}_{i,k}\right]\\
&\qquad=0.5\left[c_k+\left(\frac{a-b}{a+b}\right)^k\bar{c}_k\right],
\end{aligned}\right\}\ (k=1\ldots N),\tag{25}$$

$$\left.\begin{aligned}
&\sum_{i=1}^{3}\left[\sum_{j=1}^{M}a_{i,j}C_{i,j,k}^{(3)}+\sum_{j=1}^{M}\bar{a}_{i,j}\bar{C}_{i,j,-k}^{(3)}+b_{i,k}\right]=0\\
&\sum_{i=1}^{3}\mu_i\left[\sum_{j=1}^{M}a_{i,j}C_{i,j,k}^{(3)}+\sum_{j=1}^{M}\bar{a}_{i,j}\bar{C}_{i,j,-k}^{(3)}+b_{i,k}\right]=0\\
&\sum_{i=1}^{3}\lambda_i\left[\sum_{j=1}^{M}a_{i,j}C_{i,j,k}^{(3)}+\sum_{j=1}^{M}\bar{a}_{i,j}\bar{C}_{i,j,-k}^{(3)}+b_{i,k}\right]=0
\end{aligned}\right\}\ (k=1\ldots M),\tag{26}$$

where

$$C_{i,j,k}^{(1)}=\frac{1}{2\pi}\int_0^{2\pi}[\rho^{-1}(\omega_i(\sigma))]^j\sigma^{-k}\,d\theta,\qquad i=1,2,3;\ \ j=1\ldots M,\ \ k=\pm1\cdots\pm N,\tag{27}$$

$$C_{i,k}^{(2)}=\begin{cases}(a_0-I\mu_i b_0)/2, k=1,\\ (\bar{a}_0+I\mu_i\bar{b}_0)/2, k=-1,\\ 0, k=\pm2,\pm3,\ldots,\pm N,\end{cases}\qquad i=1,2,3;\tag{28}$$

$$C_{i,j,k}^{(3)}=\frac{1}{2\pi}\int_0^{2\pi}[\omega_i^{-1}(\rho(\sigma'))]^{-j}(\sigma')^{-k}\,d\theta',\qquad i=1,2,3;\ \ j=1\ldots N,\ \ k=\pm1\cdots\pm M.\tag{29}$$

Here, the definite integrals in Equations (27) and (29) can be evaluated numerically, for example, by Gaussian quadrature. Finally, the $(4N+3M)$ unknown coefficients $a_{i,j}$ $(i=1,2,3;\ j=1\ldots N)$, c_j $(j=1\ldots N)$ and $b_{i,j}$ $(i=1,2,3;\ j=1\ldots M)$ are determined from Equations (25) and (26), following which we can obtain the electro-elastic field in the piezoelectric half-plane and the electric field inside the elliptical hole.

4. Numerical examples

In the following examples, the material constants of the piezoelectric half-plane are taken as those of PZT-4 ceramic [Berlincourt et al. 1964],

$$\begin{aligned} a_{11} = 8.205 \times 10^{-12},\ a_{12} = -3.144 \times 10^{-12}, \quad & a_{22} = 7.495 \times 10^{-12}, \quad a_{33} = 19.3 \times 10^{-12}(\mathrm{Pa}^{-1}); \\ b_{13} = 39.4 \times 10^{-3}, \quad & b_{21} = -16.62 \times 10^{-3}, \quad b_{22} = 23.96 \times 10^{-3}(\mathrm{m}^2/\mathrm{C}); \\ & c_{11} = 7.66 \times 10^{7}, \quad c_{22} = 9.82 \times 10^{7}(\mathrm{m/F}); \end{aligned} \tag{30}$$

and the related complex parameters μ_i, λ_i and κ_i $(i = 1, 2, 3)$ in Equations (4) and (5) are calculated as

$$\begin{aligned} & \mu_1 = 1.218I, \qquad -\bar{\mu}_2 = \mu_3 = 0.201 + 1.070I; \\ & \lambda_1 = -6.351 \times 10^{-10}, \qquad \lambda_2 = \bar{\lambda}_3 = (-2.411 + 1.362I) \times 10^{-10}(\mathrm{m \cdot F/C}); \\ & \kappa_1 = -0.0113I, \qquad -\bar{\kappa}_2 = \kappa_3 = 0.0154 + 0.0203I\,(\mathrm{m}^2/\mathrm{C}); \end{aligned} \tag{31}$$

while the medium inside the elliptical hole is assumed to be homogeneous air with an approximate dielectric constant $\epsilon_0 = 8.85 \times 10^{-12}\,\mathrm{F/m}$. The convergence of the present solution is verified by the fact that the relative error between the calculated electro-elastic field corresponding to two adjacent values of N and M is less than 10^{-4}.

4.1. ***Verification of the method.*** Our solution for a piezoelectric half-plane degenerates quite simply into that for an elastic half-plane without piezoelectricity when all of the piezoelectric constants b_{ij} in Equations (4) and (5) tend towards zero. Comparisons between our present solutions and known results [Dejoie et al. 2006; Kushch et al. 2006] for stress distributions in an isotropic half-plane with circular or elliptical hole are presented in Figures 3 and 4 which indicated good agreement between the two.

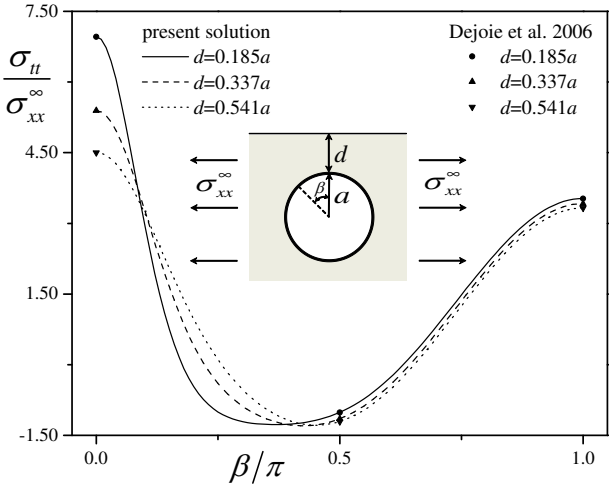

Figure 3. Hoop stress around a circular hole in an isotropic half-plane under uniform uniaxial tensile loading parallel to the edge of the half-plane.

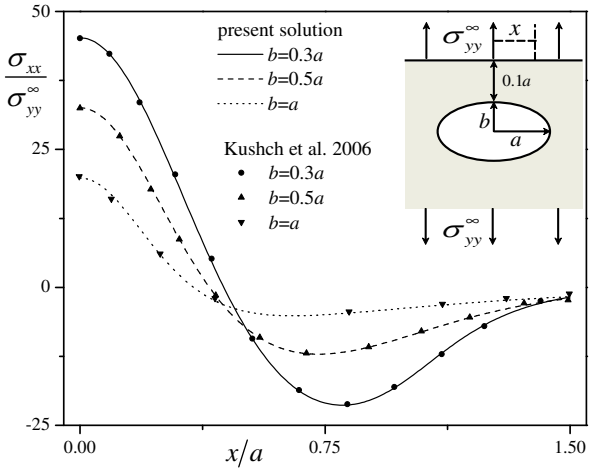

Figure 4. Stress concentration along the edge of an isotropic half-plane with an elliptical hole under uniform uniaxial tensile loading perpendicular to the edge.

4.2. ***An elliptical hole in a piezoelectric half-plane.*** Figures 5 and 6 show the hoop stresses around an elliptical hole in a piezoelectric half-plane under mechanical and electric loadings, respectively, with increasing distance between the hole and the edge of the half-plane.

In Figures 5 and 6 we see that, as the distance between the hole and the edge of the half-plane

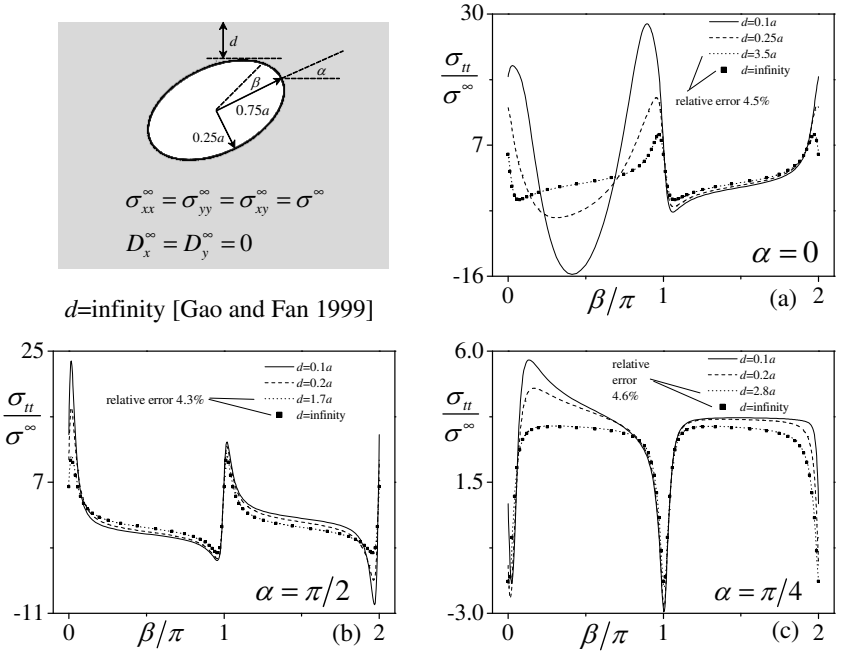

Figure 5. Hoop stress around an elliptical hole in a piezoelectric half-plane under mechanical loadings.

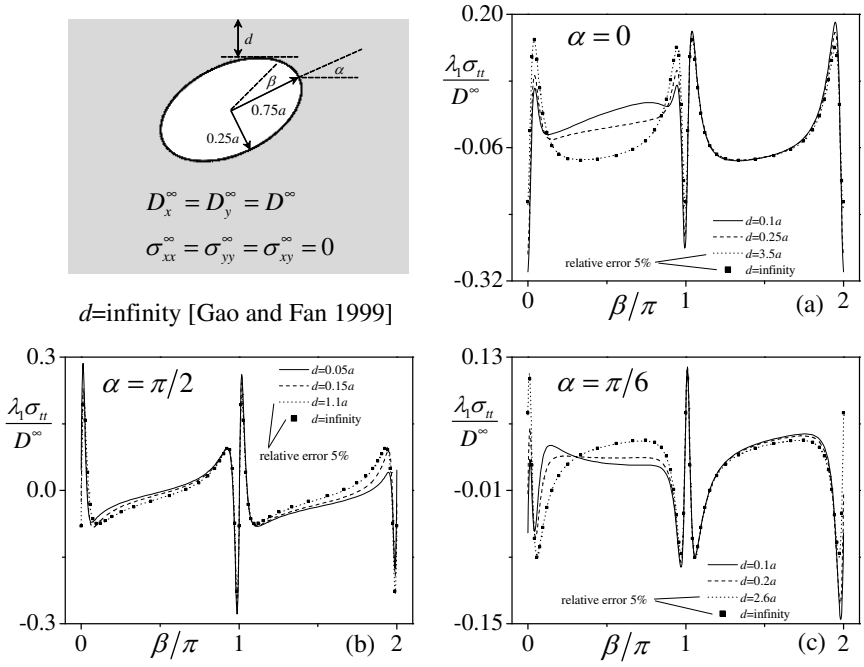

Figure 6. Hoop stress around an elliptical hole in a piezoelectric half-plane under electric loadings.

decreases, the maximum hoop stress around the hole increases rapidly under the influence of mechanical loadings but much slower when subjected to electric loading. On the other hand, for an arbitrarily-oriented elliptical hole in a piezoelectric half-plane under either mechanical or electric loading, when the distance between the hole and the edge exceeds, for example, four times the size of the hole, the effect of the edge on the stress concentration around the hole is negligible so that the half-plane can be modeled approximately as a whole plane.

4.3. ***A crack in a piezoelectric half-plane.*** Since the crack face is permeable to an electric field, electric loading alone does not induce stress or electric field concentrations at the crack tips. As a result, here we consider only mechanical loading. Stress and electric displacement intensity factors at the crack tips in a piezoelectric half-plane subjected to mechanical loading are given in Figures 7–12.

It is shown in Figures 7–12 that both stress and electric displacement intensity factors at the crack tip closest to the edge of the half-plane always increase with decreasing distance between the crack and the edge. However, as shown in Figure 11(b), for a crack with particular orientation in a piezoelectric half-plane under pure shear loading, the mode-II stress intensity factor at the crack tip farthest from the edge of the half-plane, may decrease with decreasing distance between the crack and the edge. Moreover, as shown in Figures 7–12, for a crack with an arbitrary orientation in a piezoelectric half-plane under mechanical loading, if the distance between the crack and the edge of the half-plane is larger than, for example, twice the length of the crack, the influence of the edge on the stress and electric displacement intensity factors at the crack tips is negligible so that the half-plane can again be treated approximately as a whole plane.

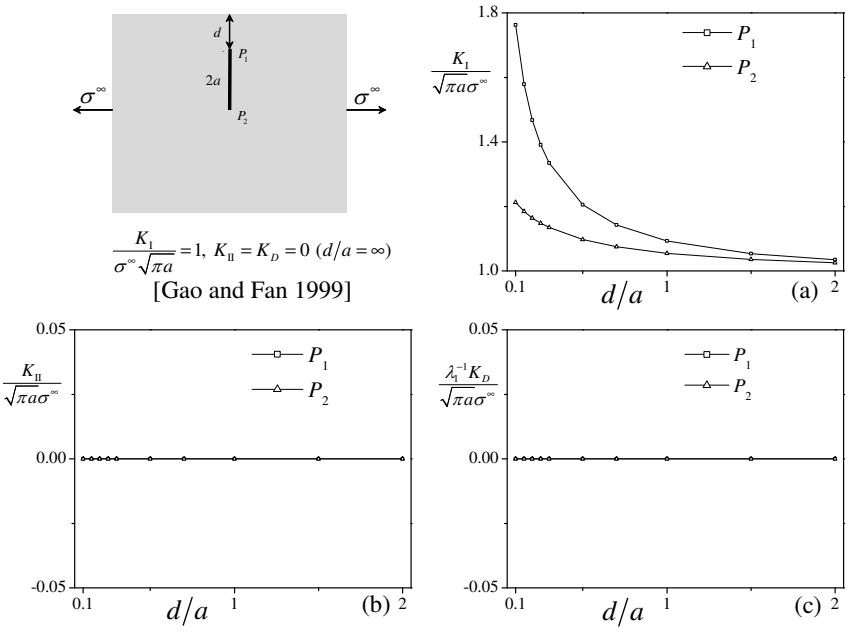

Figure 7. Intensity factors of stress and electric displacement at the tips of a crack perpendicular to the edge of the piezoelectric half-plane under uniaxial tensile loading parallel to the edge.

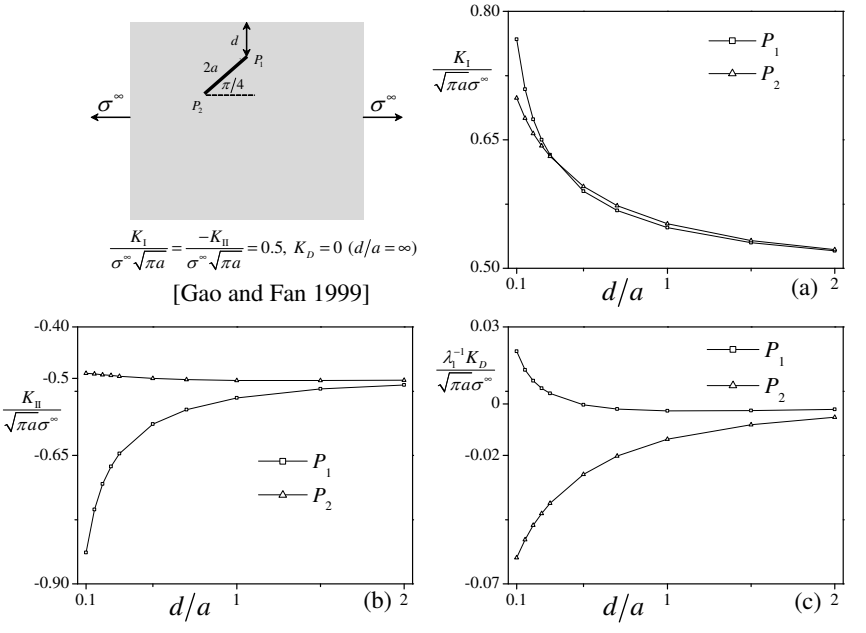

Figure 8. Intensity factors of stress and electric displacement at the tips of a crack inclined from the edge of the piezoelectric half-plane under uniaxial tensile loading parallel to the edge.

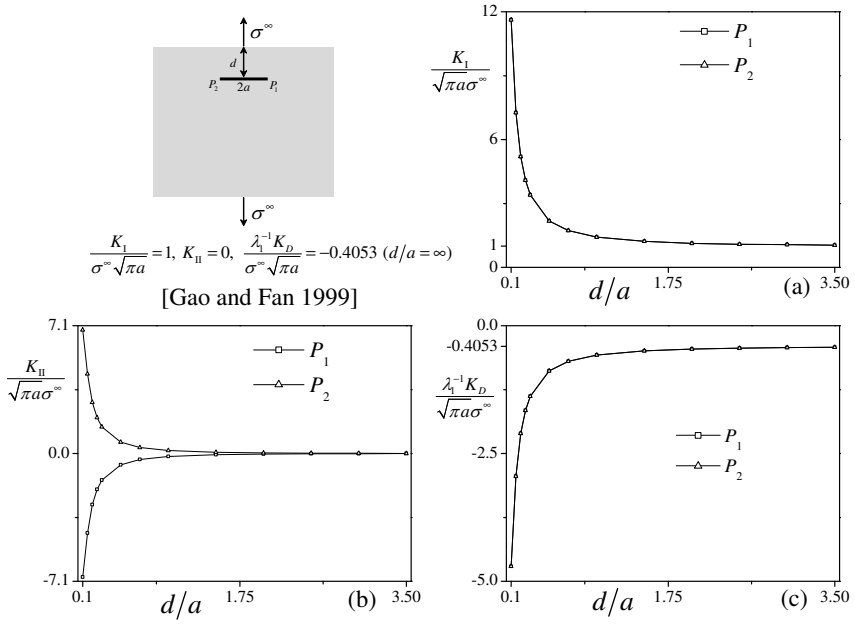

Figure 9. Intensity factors of stress and electric displacement at the tips of a crack parallel to the edge of the piezoelectric half-plane under uniaxial tensile loading perpendicular to the edge.

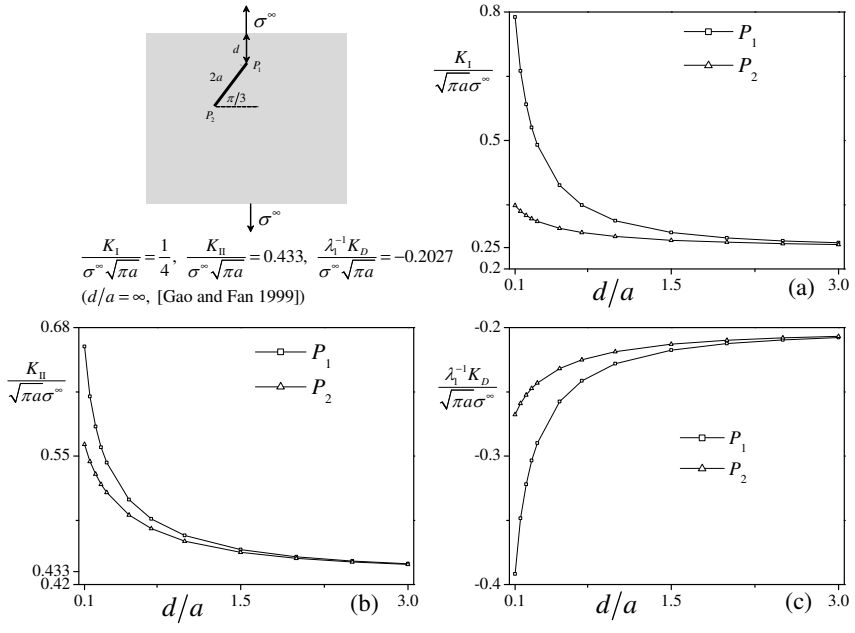

Figure 10. Intensity factors of stress and electric displacement at the tips of a crack inclined from the edge of the piezoelectric half-plane under uniaxial tensile loading perpendicular to the edge.

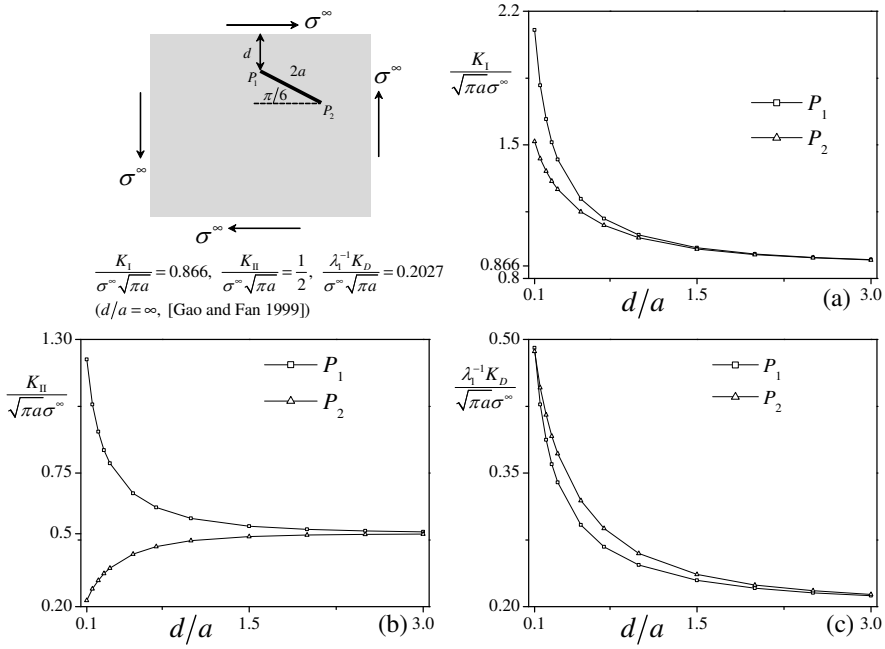

Figure 11. Intensity factors of stress and electric displacement at the tips of a crack inclined from the edge of the piezoelectric half-plane under pure shear loading.

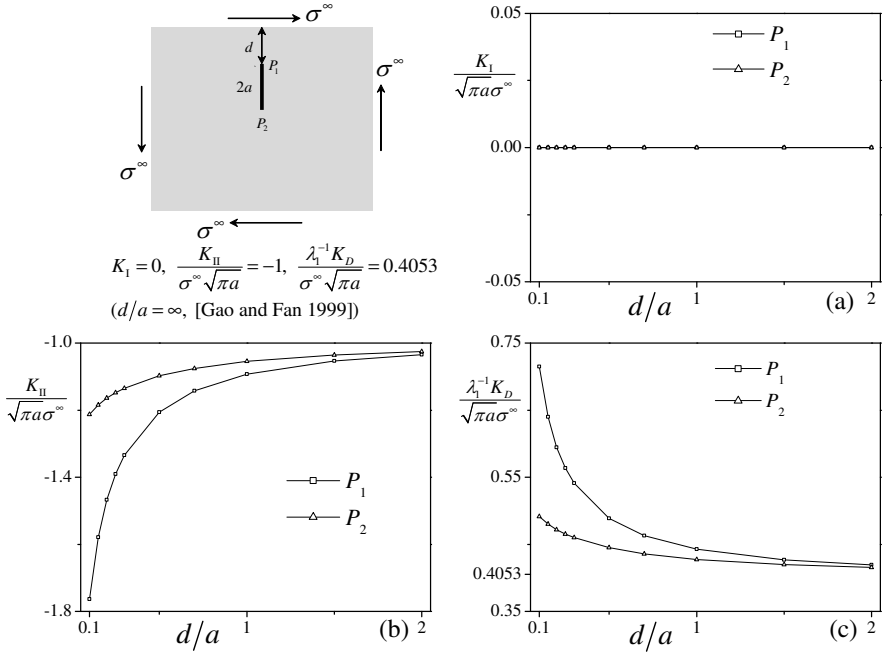

Figure 12. Intensity factors of stress and electric displacement at the tips of a crack perpendicular to the edge of the piezoelectric half-plane under pure shear loading.

5. Conclusions

The electro-elastic field in a piezoelectric half-plane containing an elliptical hole or a crack under in-plane electromechanical loadings is obtained using conformal mapping and Fourier expansion techniques. Numerical results are given to verify the feasibility of the present solution and to demonstrate the effect of the edge of the half-plane on the stress concentration around the hole and on the electro-elastic intensity factors at the crack tips. For an elliptical hole or a crack in a piezoelectric half-plane with an edge perpendicular to the poling direction of the half-plane with mechanical or electric loading imposed on the edge and remotely, our main conclusions are as follows:

(1) The maximum hoop stress around the elliptical hole increases with decreasing distance between the hole and the edge of the half-plane under either mechanical or electric loading. However, the hoop stress around the hole is much more sensitive to the distance between the hole and the edge of the half-plane when subjected to mechanical as opposed to electric loading.

(2) In general, all stress and electric displacement intensity factors at the two crack tips increase with decreasing distance between the crack and the edge of the half-plane. However, for a crack with particular orientations in a piezoelectric half-plane subjected to pure shear loading, the mode-II stress intensity factor at one of the crack tips (that farthest from the edge) may decrease with decreasing distance between the crack and the edge.

(3) When the distance between the elliptical hole or the crack and the edge of the half-plane is more than four times the size of the hole or the semi-length of the crack, the half-plane can be treated approximately as a whole plane.

Acknowledgement

Dai appreciates the support of the China Scholarship Council. Dai and Gao acknowledge the support of the National Natural Science Foundation of China (11232007&11472130) and a Project Funded by the Priority Academic Program Development of Jiangsu Higher Education Institutions (PAPD). Schiavone thanks the Natural Sciences and Engineering Research Council of Canada for their support through a Discovery Grant (Grant # RGPIN 155112).

References

[Berlincourt et al. 1964] D. A. Berlincourt, D. R. Curran, and H. Jaffe, "Piezoelectric and piezomagnetic materials and their function in transducers", pp. 169–270 in *Physical acoustics: principles and methods*, vol. 1A, edited by W. P. Mason, Academic Press, New York, NY, 1964.

[Chung and Ting 1996] M. Y. Chung and T. C. T. Ting, "Piezoelectric solid with an elliptic inclusion or hole", *Int. J. Solids Struct.* **33**:23 (1996), 3343–3361.

[Copson 1935] E. T. Copson, *An introduction to the theory of functions of a complex variable*, Oxford, London, 1935.

[Dai and Gao 2014] M. Dai and C.-F. Gao, "Perturbation solution of two arbitrarily-shaped holes in a piezoelectric solid", *Int. J. Mech. Sci.* **88** (2014), 37–45.

[Dai and Sun 2013] M. Dai and H. Sun, "Thermo-elastic analysis of a finite plate containing multiple elliptical inclusions", *Int. J. Mech. Sci.* **75** (2013), 337–344.

[Dejoie et al. 2006] A. Dejoie, S. G. Mogilevskaya, and S. L. Crouch, "A boundary integral method for multiple circular holes in an elastic half-plane", *Eng. Anal. Bound. Elem.* **30**:6 (2006), 450–464.

[Gao and Fan 1999] C.-F. Gao and W.-X. Fan, "Exact solutions for the plane problem in piezoelectric materials with an elliptic [sic] or a crack", *Int. J. Solids Struct.* **36**:17 (1999), 2527–2540.

[Guo et al. 2010] J.-H. Guo, Z.-X. Lu, H.-T. Han, and Z. Yang, "The behavior of two non-symmetrical permeable cracks emanating from an elliptical hole in a piezoelectric solid", *Eur. J. Mech. A Solids* **29**:4 (2010), 654–663.

[Kaloerov and Glushchenko 2001] S. A. Kaloerov and Y. A. Glushchenko, "Electroelastic state of a multiply connected piezoelectric half plane with holes and cracks", *J. Math. Sci.* (*NY*) **107**:6 (2001), 4416–4424.

[Kushch et al. 2006] V. I. Kushch, S. V. Shmegera, and V. A. Buryachenko, "Elastic equilibrium of a half plane containing a finite array of elliptic inclusions", *Int. J. Solids Struct.* **43**:11–12 (2006), 3459–3483.

[Lekhnitskii 1950] S. G. Lekhnitskii, *Теория упругости анизотропного тела*, Gostekhizdat, Moscow, 1950. Translated as *Theory of elasticity of an anisotropic elastic body*, Holden Day, San Francisco, CA, 1963. 2nd ed. in Russian published by Nauka, Moscow, 1977; translated by Mir, Moscow, 1981.

[Pak 2010] Y. E. Pak, "Elliptical inclusion problem in antiplane piezoelectricity: implications for fracture mechanics", *Int. J. Eng. Sci.* **48**:2 (2010), 209–222.

[Pan 2004] E. Pan, "Eshelby problem of polygonal inclusions in anisotropic piezoelectric full- and half-planes", *J. Mech. Phys. Solids* **52**:3 (2004), 567–589.

[Qin 1998] Q.-H. Qin, "Thermoelectroelastic Green's function for a piezoelectric plate containing an elliptic hole", *Mech. Mater.* **30**:1 (1998), 21–29.

[Ru 2000] C. Q. Ru, "Eshelby's problem for two-dimensional piezoelectric inclusions of arbitrary shape", *Proc. R. Soc. Lond. A* **456**:1997 (2000), 1051–1068.

[Shen et al. 2010] M. H. Shen, F. M. Chen, and S. Y. Hung, "Piezoelectric study for a three-phase composite containing arbitrary inclusion", *Int. J. Mech. Sci.* **52**:4 (2010), 561–571.

[Sosa 1991] H. Sosa, "Plane problems in piezoelectric media with defects", *Int. J. Solids Struct.* **28**:4 (1991), 491–505.

[Sosa and Khutoryansky 1996] H. Sosa and N. Khutoryansky, "New developments concerning piezoelectric materials with defects", *Int. J. Solids Struct.* **33**:23 (1996), 3399–3414.

[Ting 2000] T. C. T. Ting, "Common errors on mapping of nonelliptic curves in anisotropic elasticity", *J. Appl. Mech.* (*ASME*) **67**:4 (2000), 655–657.

[Wang and Gao 2012] Y.-J. Wang and C.-F. Gao, "Thermoelectroelastic solution for edge cracks originating from an elliptical hole in a piezoelectric solid", *J. Therm. Stresses* **35**:1–3 (2012), 138–156.

[Wang and Zhou 2013] X. Wang and K. Zhou, "Three-phase piezoelectric inclusions of arbitrary shape with internal uniform electroelastic field", *Int. J. Eng. Sci.* **63** (2013), 23–29.

[Wang et al. 2015] Y.-J. Wang, C.-F. Gao, and H. Song, "The anti-plane solution for the edge cracks originating from an arbitrary hole in a piezoelectric material", *Mech. Res. Commun.* **65** (2015), 17–23.

[Yang et al. 2007] P. S. Yang, J. Y. Liou, and J. C. Sung, "Analysis of a crack in a half-plane piezoelectric solid with traction-induction free boundary", *Int. J. Solids Struct.* **44**:25–26 (2007), 8556–8578.

[Zhang and Gao 2004] T.-Y. Zhang and C.-F. Gao, "Fracture behaviors of piezoelectric materials", *Theor. Appl. Fract. Mech.* **41**:1–3 (2004), 339–379.

Received 3 Dec 2015. Revised 21 Jan 2016. Accepted 9 Mar 2016.

MING DAI: mdai1@ualberta.ca
State Key Laboratory of Mechanics and Control of Mechanical Structures, Nanjing University of Aeronautics and Astronautics, Nanjing, 210016, China

and

Department of Mechanical Engineering, University of Alberta, Edmonton, Alberta T6G 2G8, Canada

PETER SCHIAVONE: p.schiavone@ualberta.ca
Department of Mechanical Engineering, University of Alberta, Edmonton, Alberta T6G 2G8, Canada

CUN-FA GAO: cfgao@nuaa.edu.cn
State Key Laboratory of Mechanics and Control of Mechanical Structures, Nanjing University of Aeronautics and Astronautics, Nanjing, 210016, China

JOURNAL OF MECHANICS OF MATERIALS AND STRUCTURES

msp.org/jomms

Founded by Charles R. Steele and Marie-Louise Steele

Cover photo: Mando Gomez, www.mandolux.com

See msp.org/jomms for submission guidelines.

JoMMS (ISSN 1559-3959) at Mathematical Sciences Publishers, 798 Evans Hall #6840, c/o University of California, Berkeley, CA 94720-3840, is published in 10 issues a year. The subscription price for 2016 is US $575/year for the electronic version, and $735/year (+$60, if shipping outside the US) for print and electronic. Subscriptions, requests for back issues, and changes of address should be sent to MSP.

JoMMS peer-review and production is managed by EditFLOW® from Mathematical Sciences Publishers.

PUBLISHED BY

mathematical sciences publishers

nonprofit scientific publishing

http://msp.org/

Journal of Mechanics of Materials and Structures

Volume 11, No. 4 July 2016

1559-3959(2016)11:4;1-5